IOPscience

HOME | SEARCH | PACS & MSC | JOURNALS | ABOUT | CONTACT US

Ion temperature and ∇B effects on ULF fluctuations at the magnetopause

This article has been downloaded from IOPscience. Please scroll down to see the full text article.

1996 Phys. Scr. 1996 254

(http://iopscience.iop.org/1402-4896/1996/T63/044)

The Table of Contents and more related content is available

Download details:
IP Address: 203.193.153.35
The article was downloaded on 02/12/2009 at 07:11

Please note that terms and conditions apply.

Physica Scripta. Vol. T63, 254–257, 1996

Ion Temperature and ∇B Effects on ULF Fluctuations at the Magnetopause

R. Pillay, R. Bharuthram* and G. S. Lakhina†

Department of Physics, University of Durban-Westville, Private Bag X54001, Durban, 4000, South Africa.

Received October 16, 1995, Accepted October 30, 1995

Abstract

In this paper, we present an extension of the work by Lakhina, Shukla and Stenflo (Geophys. Res. Lett. **20**, 2419 1993) on the generation of ultralow frequency (ULF) fluctuations at the earth's magnetopause. A high beta model for the generation of these short wavelength fluctuations is described. In this model, drifts due to density and magnetic field gradients, present at the magnetopause, act as free energy sources for the excitation of the ULF waves. The model also considers both warm electrons and ions and is based on the SS equations (Shukla and Stenflo. J. Exp. Theor. Phys. **57**, 692 1993) for low-frequency EM waves in non-uniform high beta magnetoplasmas. Using fluid theory the associated dispersion relation is first established, then numerically solved for unstable modes in different regions of parameter space.

1. Introduction

The magnetopause region of the earth has stimulated a lot of research into its physical processes and wave phenomena [1–3]. Work on low-frequency electromagnetic fluctuations has centered on low β plasmas [4] ($\beta = 2\mu_o n_o (T_e + T_i)/B_o^2$), where n_o is the particle number density, T_e and T_i the electron and ion temperature, respectively, and B_o the strength of the external magnetic field). However, such models do not accurately describe coherent electromagnetic wave phenomena at the earth's magnetopause since the plasma β in the solar wind and in the magnetopause region can be greater than unity [1]. Recently, Shukla and Stenflo, [5, 6] and Lakhina *et al.*, [7], have derived non-linear equations for electromagnetic waves in high β plasmas. The model of Lakhina *et al.*, [7] governs the dynamics of weakly interacting low-frequency electromagnetic modes in high β collisionless plasmas which contain an equilibrium density gradient. In this instance, the density gradient present in the magnetopause acts as a free energy source for the excitation of the waves. However, their model does not take into account the effects of magnetic field gradients and the ion temperature (i.e. they assumed the ions to be cold). In high β plasmas these effects could prove significant, especially in regions of the magnetopause where the ions are warmer than the electrons i.e. $T_i > T_e$ [2].

The model that we propose extends the work of Lakhina *et al.*, [7] in that it incorporates both the magnetic field gradient and the ion temperature. We assume that the external magnetic field $\boldsymbol{B}_o$ is directed along the $\hat{z}$ axis and that the equilibrium density gradient ∇n_o and magnetic field gradient ∇B_o are directed along the $\hat{x}$ axis in a Cartesian co-ordinate system. If we consider both warm electrons and ions, then following Lakhina *et al.*, [7] the propagation of low-frequency (in comparison with the ion gyro-frequency ω_{ci} electromagnetic waves in non-uniform high β plasmas is governed by the electron and ion continuity equations

$$\partial_t n_e + \nabla\cdot(n_e \boldsymbol{v}_{e\perp}) + \partial_z (n_e v_e z) = 0, \tag{1a}$$

$$\partial_t n_i + \nabla\cdot(n_i v_{i\perp}) + \partial_z (n_i v_i z) = 0, \tag{1b}$$

respectively, the conservation of total current in the quasi-neutrality approximation $n_e = n_i = n$,

$$\nabla\cdot\boldsymbol{j} \equiv e\,\{\nabla_\perp\cdot[n\,(\boldsymbol{v}_{i\perp} - \boldsymbol{v}_{e\perp})] + \partial_z\,[n\,(v_i z - v_e z)]\} = 0, \tag{2}$$

as well as Faraday's and Ampere's laws, respectively,

$$\partial_t \boldsymbol{B}_1 = -\nabla\times\boldsymbol{E}, \tag{3}$$

$$\nabla\times\boldsymbol{B}_1 = \mu_o \boldsymbol{j}, \tag{4}$$

where the subscript e(i) stands for electrons (ions), n_j is the total number density of the particle species j, $\boldsymbol{v}_j$ is the mean velocity, and $\boldsymbol{E}$ and $\boldsymbol{B}_1$ are the wave electric and magnetic fields, respectively.

In the drift approximation ($\omega \ll \Omega_j$), the perpendicular components of the electrons and ions fluid velocities are: $\boldsymbol{v}_{e\perp} \approx \boldsymbol{v}_E + \boldsymbol{v}_{De} + \boldsymbol{v}_{Be}$ and $\boldsymbol{v}_{i\perp} \approx \boldsymbol{v}_E + \boldsymbol{v}_{pi} + \boldsymbol{v}_{Di} + \boldsymbol{v}_{Bi}$, where $\boldsymbol{v}_E = \boldsymbol{E}\times\boldsymbol{B}_o/B_o$ is the $\boldsymbol{E}\times\boldsymbol{B}$ drift, $\boldsymbol{v}_{Dj} = \left(m_j v_{tj}^2/q_j B_o\right)\hat{z}\times\nabla\ln n_j$ and $\boldsymbol{v}_{Bj} = (\tfrac{1}{2} m\, v_{j\perp}^2/q_j B_o^3)\,\boldsymbol{B}_o\times\nabla B_o$ are the diamagnetic and $\nabla\boldsymbol{B}$ drifts of the species j ($q_j = +e(-e)$ for i(e)), and $\boldsymbol{v}_{pi} = (1/B_o\,\omega_{ci})\,\partial_t\boldsymbol{E}_\perp$ is the ion polarisation drift, $v_{tj} = (T_j/m_j)^{1/2}$ is the thermal speed of the j^{th} species, $m_i(m_e)$ and $T_i(T_e)$ the ion (electron) mass and temperature, respectively, and $\boldsymbol{E}_\perp$ is the perpendicular (to $\hat{z}$) component of the wave electric field vector.

From the momentum equation the parallel components of the electron and ion fluid velocities are, respectively,

$$\partial_t v_{ez} = -\left(\frac{e}{m_e}\right)E_z - \left(\frac{v_{te}^2}{n_e}\right)\partial_z n_e - \left(\frac{e}{m_e}\right)[(\boldsymbol{v}_{Do}\times\boldsymbol{B}_1)_z + (\boldsymbol{v}_{Bi}\times\boldsymbol{B}_1)_z], \tag{5}$$

$$\partial_t v_{iz} = \left(\frac{e}{m_i}\right)E_z - \left(\frac{v_{ti}^2}{m_i}\right)\partial_z n_i + \left(\frac{e}{m_i}\right)[(\boldsymbol{v}_{Di}\times\boldsymbol{B}_1)_z + (\boldsymbol{v}_{Bi}\times\boldsymbol{B}_1)_z + (\boldsymbol{v}_{pi}\times\boldsymbol{B}_1)_z]. \tag{6}$$

Writing $n_e = n_o(x) + n_1$, where $n_1 \ll n_o$, we have from 1(a) and 1(b)

$$\partial_t (N - b) + \boldsymbol{v}_E\cdot\ \nabla\ln n_o(x) + \partial_z\left[v_{iz} - \frac{1}{\mu_o e n_o}(\nabla\times\boldsymbol{B}_1)_z\right] = 0, \tag{7}$$

where $N = n_1/n_o$ and $b = B_{1z}/B_o$ are the relative density and compressional magnetic field perturbations, respectively.

*Also at Plasma Physics Research Institute, University of Natal, Durban 4000, South Africa.

†Indian Institute of Geomagnetism, Dr Nanabhai Moos Marg, Colaba, Bombay-400 005, India.

Equation (2) yields:

$$\partial_t \nabla \cdot \boldsymbol{E}_\perp + v_A^2 \partial_z (\nabla \times \boldsymbol{B}_1)_z = 0, \tag{8}$$

where $v_A = B_o/(\mu_o n_o m_i)^{1/2}$ is the Alfvén velocity.

Subtracting equation (6) from (5) and using equation (4) we obtain:

$$\partial_t (\nabla \times \boldsymbol{B}_1)_z = \frac{\omega_{pe}^2}{c^2}\left[\left(1 + \frac{m_e}{m_i}\right)E_z + S\partial_z N + S\left(\frac{1}{B_o}\right)\boldsymbol{B}_1 \cdot \nabla \ln n_o + S\left(\frac{1}{2}\right)\left(\frac{1}{B_o^2}\right)B_{1x}\partial_x B_o\right], \tag{9}$$

where $S = (T_e/e)[1 - (m_e/m_i)(T_i/T_e)]$ and $\omega_{pe} = (n_o e^2/\varepsilon_o m_e)^{1/2}$ is the electron plasma frequency.

From equation (4) we have:

$$\left(\frac{\partial^2}{\partial t^2} - v_A^2 \nabla^2\right) b = T\,\nabla_\perp^2 N + \left(\frac{1}{B_o^2}\right) T\,(ik_y B_{1x}\partial_x B_o), \tag{10}$$

where $T = (T_i/m_i)(1 + T_e/T_i)$.

Also from equation (3) we obtain:

$$\partial_t (\nabla \times \boldsymbol{B}_1)_z = \nabla_\perp^2 E_z - \partial_z \nabla \cdot \boldsymbol{E}_\perp. \tag{11}$$

We derive the dispersion relation by assuming that all physical variables vary as $e^{i(\mathbf{k}\cdot\mathbf{r} - \omega t)}$, where ω and $\boldsymbol{k} = \boldsymbol{k}_\perp + \hat{z}\,k_z$ are the wave frequency and wave vector, respectively.

Equation (7) to (10) then transforms as follows:

$$\frac{i\kappa}{B_o} E_y + \omega(N - b) = ik_z\left[\frac{e}{m_i \omega}E_z - \frac{1}{\mu_o e n_o}(\boldsymbol{k} \times \boldsymbol{B}_1)_z\right], \tag{12}$$

$$\omega \boldsymbol{k} \cdot \boldsymbol{E}_\perp = k_z v_A^2 (\boldsymbol{k} \times \boldsymbol{B}_1)_z, \tag{13}$$

$$\omega(\boldsymbol{k} \times \boldsymbol{B}_1)_z = \frac{\omega_{pe}^2}{c^2}\left[\left(1 + \frac{m_e}{m_i}\right)E_z + S\,ik_z N + \left(\frac{S}{\omega B_o}\right)(k_y E_z - k_z E_y)\left(\kappa + \frac{1}{2}\varepsilon_B\right)\right], \tag{14}$$

$$(\omega^2 - k^2 v_A^2) b = T k_\perp^2 N + \left(\frac{1}{\omega B_o}\right) T\, ik_y\, \varepsilon_B (k_y E_z - k_z E_y), \tag{15}$$

where $\kappa = d_x \ln n_o(x)$ and $\varepsilon_B = d_x \ln B_o(x)$ are the expressions for the density and magnetic field gradients, respectively.

Fourier transformation of equation (11) yields:

$$\omega(\boldsymbol{k} \times \boldsymbol{B}_1)_z = -(k_\perp^2 E_z - k_z \boldsymbol{k} \cdot \boldsymbol{E}_\perp). \tag{16}$$

Combining equation (12) to (16) we obtain the dispersion relation:

$$A_1 B_2 - A_2 B_1 = 0, \tag{17}$$

where

$$A_1 = \left[i\kappa k_x \overline{C}_s^2 + \left[(\omega^2 - k^2 v_A^2) - k_\perp^2 \overline{C}_s^2\right] - \frac{ik_x k_y k_z \varepsilon_B \overline{C}_s^2}{k_\perp^2}\right],$$

$$A_2 = \frac{1}{(\omega^2 - k_z^2 v_A^2)}\{[(\omega^2 - k^2 v_A^2) - k_\perp^2 \overline{C}_s^2] k_y k_z v_A^2 + ik_x k_y^2 \varepsilon_B \overline{C}_s^2 (\omega^2 - k_z^2 v_A^2) - i\frac{\omega_{ci}}{\omega} k_x k_z \overline{C}_s^2 [\omega^2(1 + k_\perp^2 \lambda_i^2) - k_z^2 v_A^2]\},$$

$$B_1 = \left[\overline{X}\left\{k_z \kappa + \frac{1}{2}k_z \varepsilon_B - \frac{ik_z(\omega^2 - k^2 v_A^2)}{k_x \overline{C}_s^2}\right\} - \frac{k_y k_z^2 \varepsilon_B \overline{C}_s^2}{k_\perp^2}\right],$$

$$B_2 = -\left[\frac{\omega^2 k_\perp^2 \lambda_e^2}{(\omega^2 - k_z^2 v_A^2)} + \left(1 + \frac{m_e}{m_i}\right) + \overline{X}\left\{\kappa k_y + \frac{1}{2}\varepsilon_B k_y + ik_z^2 \frac{(\omega^2 - k^2 v_A^2)}{(\omega^2 - k_z^2 v_A^2)}\frac{k_y v_A^2}{k_x \overline{C}_s^2} - \frac{k_y^2 k_z \varepsilon_B}{k_\perp^2}\right\}\right],$$

with $\overline{C}_s^2 = T_e/m_i + T_i/m_i$, $\overline{X} = (C_s^2/\omega\omega_{ci})(1 - T\frac{m_e}{m_i})$, and $C_s = (T_e/m_i)^{1/2}$ is the ion sound speed. The dispersion relation (17) reduces to a sixth order polynomial in ω.

2. Numerical Results

We have solved the dispersion relation (17) numerically using typical magnetopause parameters [7]. In all the graphs plotted the frequency ω has been normalised by the ion cyclotron frequency, $\omega_{ci} = \frac{eB_o}{m_i}$, speed by the Alfvén velocity v_A and the wave number k by $\frac{v_A}{\omega_{ci}}$. The results are displayed in Figures 1–7.

Fig. 1 shows the case in which both density and magnetic field gradients are absent (i.e. $\varepsilon = 0$ and $\eta = 0$), where ε and η are the normalised density and magnetic field gradients, respectively. We also assume the ions to be cold. In this case there is no free energy source to drive the modes unstable [5]. Therefore all six modes are found to be real, as expected. The six modes (labelled 1–6) constitute three pairs, equal in magnitude but opposite in sign, as found by Shukla and Stenflo, [5]. As pointed out by them, these ULF modes arise from the coupling of the shear Alfvén wave and the magnetosonic wave.

Fig. 2 shows the effect that a finite density gradient ($\varepsilon \neq 0$) has on the real frequencies of the modes. In this case we assume the absence of any magnetic field gradients and that the ions are cold. The presence of a density gradient provides a energy source to destablise some of the modes. Modes 3, 5 and 6 are found to be unstable for the parameters chosen (see Fig. 3). For a fixed wavelength (k constant) an increase in the density gradient (ε) causes the real frequencies of modes 3 and 5 to decrease and increase, respectively, but has little effect on mode 6. In Fig. 2 mode 6 has almost unit slope and is identified as the predominant shear Alfvén mode. Curve 5, which is most sensitive to the change in ε experiences the effect of the "diamagnetic (∇n) drift mode."

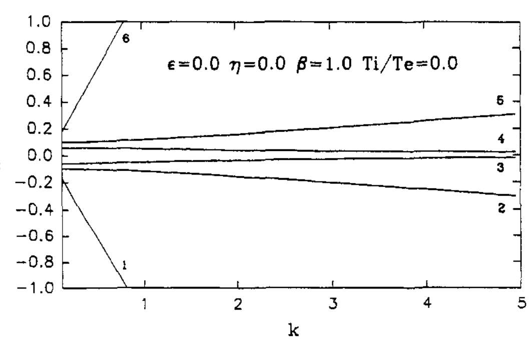

Fig. 1. Solution of the dispersion relation (17) for the parameters: $\beta = 1.0$, $k_x = k_z = 0.1$, $\frac{T_i}{T_e} = 0$, $\eta = \frac{|\varepsilon_B|\, v_A}{\omega_{ci}} = 0$ and $\varepsilon = \frac{|\kappa|\, v_A}{\omega_{ci}} = 0$ (i.e. the uniform plasma case).

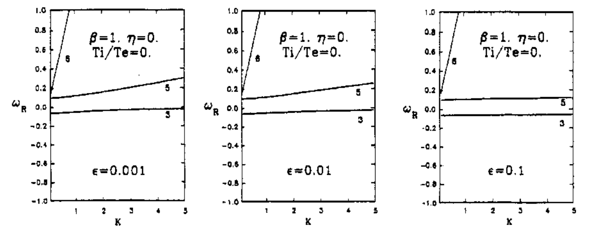

Fig. 2. Solution of the dispersion relation for the parameters: $\beta = 1.0$, $k_x = k_z = 0.1$, $\frac{T_i}{T_e} = 0$, $\eta = 0$ and $\varepsilon = 0.001, 0.01, 0.1$.

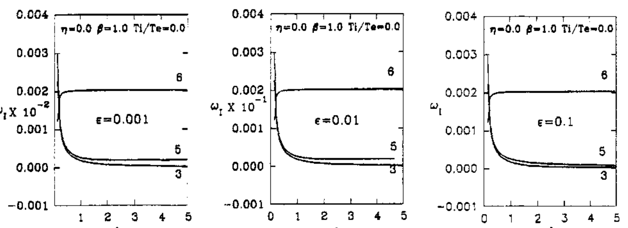

Fig. 3. The variation of the growth rate of the modes 3,5,6 for the parameters in Fig. 2.

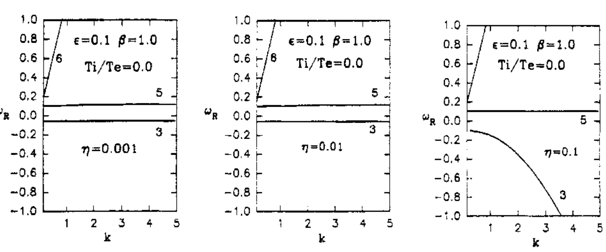

Fig. 4. The variation of the real frequencies, ω_R, of the modes 3,5,6 corresponding to a changing magnetic field gradient η. The parameters are: $\beta = 1.0$, $k_x = k_z = 0.1$, $\frac{T_i}{T_e} = 0$, $\varepsilon = 0.1$ and $\eta = 0.001, 0.01, 0.1$.

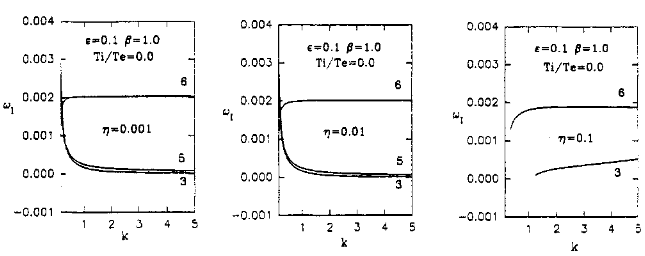

Fig. 5. The variation of the growth rate of the modes 3,5,6 for the parameters in Fig. 4.

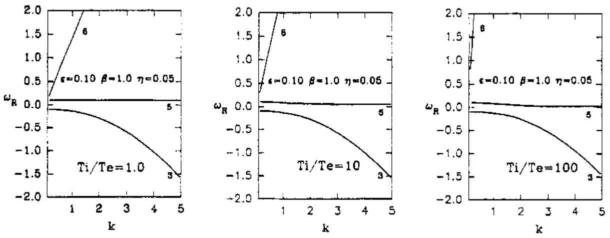

Fig. 6. The variation of the real frequencies, ω_R, of the modes 3,5,6 for different ion temperatures. The magnetic field gradient η and density gradient ε are fixed at 0.05 and 0.1, respectively. The parameters are: $\beta = 1.0$, $k_x = k_z = 0.1$, $\frac{T_i}{T_e} = 1.0, 10.0, 100.0$.

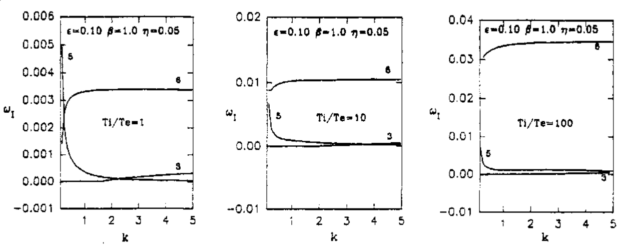

Fig. 7. The variation of the growth rate of the modes 3,5,6 for different ion temperatures. The fixed parameters are the same as in Fig. 6.

Fig. 3 shows the growth rate (γ) of the unstable modes 3,5 and 6. We see that the growth rate is more sensitive to changes in density than the real frequency, increasing as ε increases. It is seen that an order of magnitude increase in ε produces a corresponding increase in the growth rate γ. For large k values, the figure shows that the stability of mode 5 is affected the most by a changing density gradient. As the wave number increases, the growth rate γ becomes independent of k for all three modes. We note that only the modes with positive group velocity (i.e. $v_g = \frac{d\omega}{d\kappa} > 0$) in Fig. 1 are unstable.

In Fig. 4 we assume the presence of both density and magnetic field gradients. The ions are still assumed to be cold. In this instance we fix the density gradient ε and vary the magnetic field gradient η. The figure shows that for small values of η there is little effect on the real frequencies of the unstable modes 3, 5 and 6. However, for $\eta > 0.1$ the real frequencies of mode 3 are found to be significantly affected, becoming larger in magnitude with increasing η for a fixed k, due to the influence of the "∇B drift mode."

Fig. 5 clearly shows the sudden increase in the growth rate of mode 3 when $\eta \geq 0.1$. As the wave number k increases, its growth becomes linear. The growth of modes 5 and 6 are not significantly affected by an η variation.

We now include the effect of finite ion temperature T_i in Fig. 6. We have set the normalised density and magnetic field gradient to be 0.1 and 0.05, respectively, and the electron temperature T_e at 25 eV, a realistic magnetopause value, and vary T_i. In this instance the real frequency of mode 6 is affected the most, increasing rapidly with increasing ion temperature.

Fig. 7 shows the significant enhancement of the growth of the mode 6 as the ion temperature increases. It dominates the instability spectrum for $T_i/T_e > 1.0$.

3. Summary

In this paper we have examined the effects of a finite ion temperature and a magnetic field gradient on ULF electromagnetic modes in a high β plasma. Of the six modes, only the three with a positive group velocity are found to be unstable. Our results show that the shear Alfvén mode is most affected by $T_i \neq 0$, while the other two modes are separately affected by $\nabla n \neq 0$ (mode 5) and $\nabla B \neq 0$ (mode 3). The enhancement in growth rate of the shear Alfvén mode is significant for increasing T_i. A similar behaviour is found for modes 3 and 5 as the inhomogeneity increases.

References

1 Labelle, J. and Treumann, R. A. Space Science Rev. **47**, 175 (1998).
2 Paschmann, G., *et al.* Space Science Rev. **22**, 717 (1978).
3 Rezeau, L., Roux, A. and Russel, C. T. J. Geophys. Res. **98**, 179 (1993).
4 Strauss, H. R., Phys. Fluids **19**, 134 (1976).
5 Shukla, P. K. and Stenflo, L. J. Exp. Theor. Phys. Lett. **57**, 692 (1993).
6 Stenflo, L. and Shukla, P. K. Physica Scripta **48**, 370 (1993).
7 Lakhina, G. S., Shukla P. K. and Stenflo, L. Geophys. Research Lett. **20**, 2419 (1993).